Inter-Research Science Publisher

Marine Ecology Progress Series
Volume 771:89–104

Published October 16, 2025
https://doi.org/10.3354/meps14953

Insights into the trophic ecology of *Etmopterus molleri*, one of the smallest shark species: a multi-tracer analysis

David Mboglen[1,2], Narcisse Ebango Ngando[3], Xinyu Chen[1], Yunkai Li[1,4,5,*]

[1]College of Marine Living Resource Sciences and Management, Shanghai Ocean University, 999 Huchenghuan Rd., 201306 Shanghai, PR China

[2]Specialized Research Station on Marine Ecosystems, Institute of Agricultural Research for Development (IRAD), 219 Kribi, Cameroon

[3]Department of Oceanography, Institute of Fisheries and Aquatic Sciences, University of Douala, 7236 Douala, Cameroon

[4]The Key Laboratory of Sustainable Exploitation of Oceanic Fisheries Resources, Ministry of Education, 999 Huchenghuan Rd., 201306 Shanghai, PR China

[5]National Engineering Research Centre for Oceanic Fisheries, Shanghai Ocean University, 999 Huchenghuan Rd., 201306 Shanghai, PR China

ABSTRACT: Deepwater sharks represent nearly half of all known shark species but aspects of their biology and ecology remain poorly understood, largely due to challenges associated with their complex life cycle, habitat, and extreme environmental conditions. The slendertail lanternshark *Etmopterus molleri* (Whitley, 1939) is one of the smallest deepwater sharks, and information on many aspects of its ecology remains scarce or non-existent to date. Here, we used a multi-tracer approach that included stomach content analysis, stable isotopes analysis ($\delta^{13}C$ and $\delta^{15}N$), and total mercury (THg) measurements in muscle and liver tissues to characterize diet and trophic ecology at 3 different life stages — juvenile, subadult, and adult. Stomach content analysis revealed that juveniles primarily consumed euphausiids, while subadults and adults shifted to mesopelagic teleosts, crustaceans, and cephalopods. Ontogenetic shifts in dietary habits were linked to increases in $\delta^{15}N$ and THg levels, and an increase in isotopic niche width. These findings suggest that *E. molleri* undergoes a progressive transition to higher trophic levels and adopts a more generalist diet as it matures. Combined with pronounced differences in niche overlap among life stages, this suggests intraspecific trophic partitioning of prey and habitats. However, further studies are needed to confirm this observation. Our study provides the first comprehensive assessment of the trophic ecology of *E. molleri,* highlighting the importance of using multiple tracers to understand the feeding strategies of deepwater sharks.

KEY WORDS: Deepwater shark · East China Sea · Feeding ecology · Stable isotopes · Stomach content · Mercury · Ontogenetic diet shift · Slendertail lanternshark

1. INTRODUCTION

Deepwater ecosystems are characterized by complex trophic networks exhibiting diverse feeding strategies, primarily dependent on energy transfer from productive epipelagic zones to near-bottom environments (Bergstad et al. 2003, Drazen & Sutton 2017, Shipley et al. 2017). Within these deep-water ecosystems, sharks function as key meso predators, regulating lower trophic levels (Heupel et al. 2014) and significantly contributing to food web stability and energy transfer within communities (Heithaus 2004, Du et al. 2022). However, overfishing threatens more than 99% of deepwater sharks and rays (where threat was assessed), with 87.7% of them being caught as bycatch (Bailey et al. 2009, Dulvy et al.

*Corresponding author: ykli@shou.edu.cn

2021, Finucci et al. 2024), followed by habitat loss and degradation (Dulvy et al. 2014, Jorgensen et al. 2022). This vulnerability is particularly concerning given their distinctive life history traits, characterized by slow growth, late maturity, and low fecundity (Cortés 1999, Norse et al. 2012). The decline of these keystone species could destabilize trophic webs, potentially altering deepwater ecosystem structure and function (Ferretti et al. 2010).

The East China Sea (ECS) continental shelf represents one of China's most productive fishing grounds, contributing approximately 40% of total fish landings (Li & Zhang 2012, Teh et al. 2019, Wang et al. 2022). This ecoregion harbors significant shark biodiversity, with 144 recorded species, and accounts for 44% of China's total shark catches (Zhang 2005, Du et al. 2022). Despite their ecological significance, there are few data on shark ecology and habitat use, which is a challenge for implementing effective conservation and management strategies (Ohshimo et al. 2016, Yano et al. 2020, Xu et al. 2022). Small deepwater species are often hindered by their low economic value, logistical constraints related to accessibility, and consequently limited research investment (Dulvy et al. 2014, Feng et al. 2022). These limitations have resulted in significant knowledge gaps regarding the dietary patterns, life history traits, and behavioral ecology of sharks (Churchill et al. 2015, Reum et al. 2020).

The slendertail lanternshark *Etmopterus molleri* (Whitley, 1939), one of the smallest (reaching up to 460 mm) and most understudied shark species, inhabits the deepwater of the Western Pacific (Last & Stevens 2009, Ebert et al. 2013). It constitutes bycatch of commercial bottom trawlers that target deepwater fishes and crustaceans in the ECS fisheries, and is routinely discarded. Consequently, this species is absent from fishing statistics, and fundamental aspects of its ecology remain unknown (Kyne et al. 2015, Mboglen et al. 2024, 2025). Research on congeners, particularly *E. spinax* and *E. pusillus*, has demonstrated that lanternsharks vary their diet during diel vertical migrations and with changing ontogeny (Neiva et al. 2006, Kousteni 2021). This could facilitate the transfer of organic matter and energy between water depths (Xavier et al. 2012, Besnard et al. 2022).

Traditionally, research has used stomach content analysis (SCA) to develop trophic models within an ecosystem (Hyslop 1980, Kolasinski et al. 2009). However, the limitations associated with the SCA approach, such as empty stomachs providing no data, the content reflecting only a snapshot of the diet, and the need for large sample sizes, can restrict its effectiveness (Daly et al. 2013, Amundsen & Sánchez-Hernández 2019). Therefore, employing a multiple-method approach that both addresses the issues of SCA and maximizes the value of small sample size is necessary to better understand shark trophic ecology (Shiffman et al. 2012, Carlisle et al. 2021).

Advances in biogeochemical tracers, particularly stable isotope analysis (SIA) and mercury (Hg), have revolutionized our understanding of marine trophic ecology by providing integrated, time-averaged indicators of foraging habits and trophic positions based on consumer tissue composition (Post 2002, Hussey et al. 2012, Le Croizier et al. 2020). Natural variations in stable isotope ratios, particularly nitrogen ($\delta^{15}N$: $^{15}N/^{14}N$) and carbon ($\delta^{13}C$:$^{13}C/^{12}C$), are used mainly to understand the structure and functioning of food webs, as well as species and community dynamics (Reum et al. 2017, Pethybridge et al. 2018, Priester et al. 2024). $\delta^{15}N$ values are typically enriched in consumers (~2–4‰) relative to their diet (Dalerum & Angerbjörn 2005, Hyodo et al. 2010) and are often used to infer trophic position and characterization of trophic niche (Post 2002, Hussey et al. 2014). $\delta^{13}C$ values change very little as carbon moves through food webs (enrichment of ~0.5–1‰) (Ishikawa et al. 2013, Manlick & Newsome 2022), reflecting the main sources of carbon and major pathways of energy transfer in the food web (Vander Zanden & Rasmussen 2001, Hussey et al. 2010, Linnebjerg et al. 2016).

On the other hand, the marine environment readily spreads mercury from terrestrial inputs, a potent pollutant and neurotoxin that tends to accumulate and biomagnify through the food web (Lavoie et al. 2013, Hilgendag et al. 2022). In the deep environments where mercury concentrations increase with depth due to methylation and sedimentation processes (Blum et al. 2013, Lamborg et al. 2014), trophic interactions become a major determinant of contaminant burdens. Although the mechanisms governing mercury bioaccumulation in fishes, particularly in deepwater elasmobranchs, remain poorly understood, dietary uptake and respiratory absorption are presumed to be the primary pathways of mercury contamination in marine predators, making the assessment of trophic interactions a crucial tool to understand contamination patterns (Pethybridge et al. 2010, Zheng et al. 2019). As a result, top trophic level predators are exposed to a greater risk of exposure to high mercury concentrations (Lavoie et al. 2013, Zhang et al. 2020, Li et al. 2022). Thus, total mercury (THg) concentration in shark tissues has emerged as a valuable tool for investigating trophic relationships, as mercury signatures can reflect trophic position (Pethybridge et al. 2012, Kiszka et al. 2015, Goyanna et al. 2023). When com-

bined with SIA, these complementary tracers provide robust insights into aspects of feeding ecology including ontogenetic dietary shifts, mercury bioaccumulation, trophic position, and habitat use (Bird et al. 2018, Bezerra et al. 2021, Riesgo et al. 2023).

In this study, we applied a combined approach of SCA with complementary biochemical tracers (SIA and THg) to investigate ontogenetic variation in the diet, trophic position, and ecological function of *E. molleri* across life stages (juvenile, subadult, and adult). Specifically, this research addressed 3 main objectives: (1) characterize the diet composition and feeding strategy of *E. molleri* through SCA, providing baseline data on prey diversity and feeding preferences; (2) determine the trophic position and foraging habitat of the species using SIA; and (3) assess mercury bioaccumulation patterns both as a validation of trophic position and as an indicator of vertical habitat use within the deepwater zone.

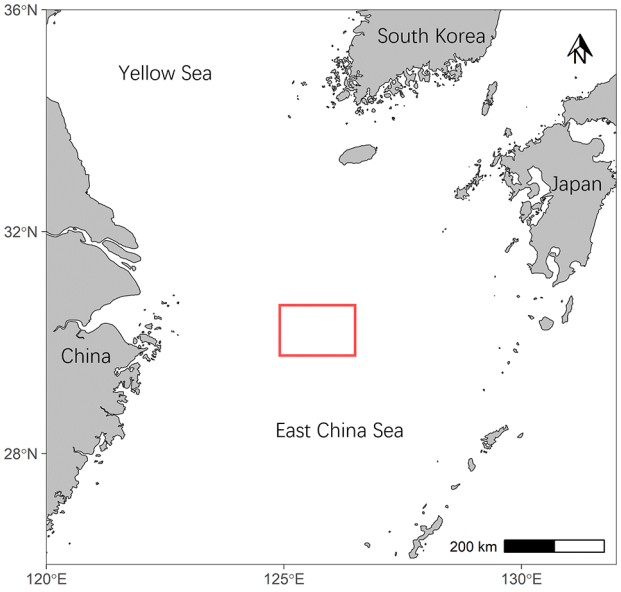

Fig. 1. Area in the East China Sea sampled for *Etmopterus molleri*. The red rectangle indicates the collection zone

2. MATERIALS AND METHODS

2.1. Sampling

Between January and April 2023 and between February and April 2024, *Etmopterus molleri* samples and potential prey were collected as bycatch from commercial bottom trawling operations in the northern boundary of the continental shelf in the ECS (Fig. 1), using nets with a codend mesh size of 40 mm primarily targeting deepwater species between 300 and 400 m deep. Following each haul, shark specimens and their potential prey were separated from the rest of the catch, appropriately labeled and frozen until further analysis. Shark individuals were visually identified to species following Ebert et al. (2021a), and a subset of 16 individuals was randomly selected across the size range for DNA confirmation. Shark muscle tissue (approximately 0.5 cm^3) was excised and rinsed thoroughly with sterile water to remove surface mucus and contaminants. Genomic DNA was extracted using a marine animal tissue DNA extraction kit (Tiangen Biotech), following the manufacturer's instructions. The mitochondrial cytochrome c oxidase subunit I (COI) gene was amplified using a pair of universal primers. The PCR products were then sequenced by Sangon Biotech Company (Shanghai, China), and sequences were compared to reference data in the NCBI GenBank database using BLAST. All individuals showed high similarity with known *E. molleri* sequences, thereby confirming the morphological identification.

For each individual, total length (TL) was measured to the nearest 0.1 mm, and the total weight was measured to the nearest 0.1 g. Sharks were sexed (presence or absence of claspers on males and females, respectively) and 3 life stages were determined following Stehmann (2002): juvenile males present claspers with a smaller length than the inner side of the pelvic fin whilst in females, the ovaries are small with a gelatinous or granulated internal structure, and no oocytes are differentiated; in subadult males, the claspers become wider, longer, and slightly exceed the length of the pelvic fins, though their skeleton remains flexible, and females at this stage show slightly enlarged ovaries with more transparent walls and differentiated oocytes of various small sizes; adult males display large claspers that are rigid and calcified, extending well beyond the pelvic fins with cartilaginous components in their deployable tips, and in females, the ovaries are large, rounded, and easily counted and measured, with well-differentiated oocytes and the presence of egg cases in the uteri, indicating full maturity. Additionally, representative prey taxa were collected during the second sampling campaign (February—April 2024).

2.2. SCA

We separated the stomachs of each shark subclass and preserved them in a 7% formalin solution. Before identifying the prey species, the stomach contents

were immersed in water for 24 h. When prey fragments were found, they were tallied and grouped together based on their morphological description (less digested or undigested component) to avoid overestimation of the frequency of a specific prey (items). We then weighed, photographed, and identified all prey items to the lowest possible taxonomic level.

The vacuity index (%VI) was calculated as %VI = $A/B \times 100$, where A is the number of empty stomachs and B is the total number of examined stomachs. Dietary indices for the different life stages were calculated using pooled stomach content data to assess the relative contribution of each prey item (i) to the species' overall diet: prey-specific abundance by number (%PN_i), prey-specific abundance by weight (%PW_i), and frequency of occurrence (%FO_i) (Hyslop 1980). Subsequently, the prey-specific index of relative importance (PSIRI) was calculated (Brown et al. 2012) by the formula:

$$\mathrm{PSIRI} = \frac{\%FO_i(\%PN_i + \%PW_i)}{2} \quad (1)$$

2.3. SIA

We used samples of shark white muscle and liver for SIA, in addition to subsamples of muscle tissues from potential prey, including fish dorsal muscle tissue (without skin), shrimp abdominal muscles, and edible cephalopod muscles. Potential prey species were selected based on stomach content observations from the 2023 survey, with additional support from the findings of Besnard et al. (2022) and Graça Aranha et al. (2023), who investigated congeners of *E. molleri*. Samples were freeze-dried at −60°C for 48 h and milled into a fine powder. We performed chemical extractions on both liver and muscle samples due to 2 major factors affecting stable isotope values in elasmobranchs: (1) high lipid content and (2) presence of osmolytes (urea and trimethylamine oxide) in tissues. These compounds can artificially deplete $\delta^{13}C$ values (lipids) and $\delta^{15}N$ values (osmolytes) (Kim et al. 2012, Logan & Lutcavage 2010, Post 2002). Lipids were extracted using a 2:1 chloroform:methanol solution, while osmolytes were removed using deionized water, following the protocol described by Li et al. (2016). Lipid extraction was solely performed for mesopelagic fish, as invertebrate species have low lipid levels (deVries et al. 2015, Hewitt et al. 2021). We weighed and encapsulated approximately 1.5 mg of defatted powder in tin cups, then fed it into a stable isotope mass spectrometer (IsoPrime 100) and elemental analyzer (vario ISOTOPE cube) at Shanghai Ocean University. The $\delta^{13}C$ and $\delta^{15}N$ values were calculated using the following equation:

$$\delta(X) = (R_{\mathrm{sample}} / R_{\mathrm{Standard}} - 1) \times 1000\ (‰) \quad (2)$$

where X is ^{13}C or ^{15}N; R_{sample} and R_{standard} are the isotope ratios of the sample and the standard sample, respectively (Li et al. 2016). The standard references used were Pee Dee belemnite for carbon and atmospheric N_2 for nitrogen. A laboratory reference (Elemental Microanalysis Protein Standard OAS, −26.98‰ for carbon, and 5.94‰ for nitrogen) was used to calibrate every 20 samples. Both analytical errors of $\delta^{13}C$ and $\delta^{15}N$ values were lower than ±0.20‰.

The trophic position (TP) of consumers was determined following the scaled framework proposed by Hussey et al. (2014), based on the $\delta^{15}N$ data calculated in Eq. (2):

$$\mathrm{TP} = \frac{\log(\delta^{15}N_{\mathrm{lim}} - \delta^{15}N_{\mathrm{zooplankton}}) - \log(\delta^{15}N_{\mathrm{lim}} - \delta^{15}N_{\mathrm{shark}})}{k} + \mathrm{TP}_2 \quad (3)$$

where $\delta^{15}N_{\mathrm{lim}}$ is the saturating isotope limit as TP increases (Hussey et al. 2014) and is calculated as the negative ratio of the intercept to the slope ($-\beta_0/\beta_1$). The intercept (β_0) and slope (β_1) values were 5.92 and −0.27, respectively, as reported by Hussey et al. (2014). According to Zou et al. (2022), the ECS baseline $\delta^{15}N$ value is 7.73‰ corresponding to mixed marine zooplankton, which are assumed to occupy the second trophic position (TP_2). $\delta^{15}N_{\mathrm{zooplankton}}$ and $\delta^{15}N_{\mathrm{shark}}$ represent the directly measured $\delta^{15}N$ values for each specimen of interest, including *E. molleri* and its potential prey items, and k is the rate at which $\delta^{15}N_{\mathrm{TP}}$ approaches $\delta^{15}N_{\mathrm{lim}}$ per trophic position, $k = -\log((\beta_0 - \delta^{15}N_{\mathrm{lim}}) / -\delta^{15}N_{\mathrm{lim}})$.

2.4. THg analysis

We only examined shark and prey tissues that had not undergone lipid extractions because it is unclear how a 2:1 chloroform:methanol solution affects mercury concentration (Guo et al. 2023). THg concentrations were determined via thermal decomposition (combustion), amalgamation, and atomic absorption spectrometry using a calibrated Direct Mercury Analyzer (DMA-80, Milestone). Approximately 20 mg dried and crushed samples of each tissue (liver and muscle) were introduced into the DMA-80. The samples underwent a drying process followed by combustion at 650°C in an oxygen-

rich environment; the analytical protocol consisted of a 100 s drying phase, a 150 s decomposition phase, and a 10 s waiting period. To ensure data quality and reliability, quality control measures included the analysis of laboratory method blanks, duplicate tissue samples, and certified reference materials (DORM-4), as described by Li et al. (2022). The precision of the analysis, as determined by duplicate sample measurements, averaged 16.56%. The precision of the method was validated through the analysis of certified reference materials, with percentage recoveries ranging from 95 to 100%.

2.5. Data analysis

We classified individual sharks into 3 life stages based on size (TL) and sexual maturity: juveniles (TL ⩽ 189.9 mm); subadults (TL 190—269.9 mm); and adults (TL ⩾ 270 mm). This classification follows the work of Ebert et al. (2021b) and Mboglen et al. (2025), which specify size at first maturity and growth curves. To determine whether diet composition differed among life stages, we used a multivariate analysis of similarity (ANOSIM) using Euclidean dissimilarity matrices with 9999 permutations. If the results were found to be significant, then post hoc analyses (pairwise comparisons) were applied to determine the specific differences with non-metric multidimensional scaling visualization based on the number of prey items. To assess the assumption of similar group dispersions, a permutational analysis of multivariate dispersions was also performed.

The trophic niche characteristics (niche width, niche size, and niche overlap) were estimated for different life stages of the sharks using both SCA and SIA results. Using SCA, the niche breadth was calculated through Levins' index (Colwell & Futuyma 1971) expressed as $B = 1/\sum p_j^2$, where B is Levins' measure of niche breadth and P_j is the proportion of individuals found in or using resource state j or the fraction of items in the diet that are of food category j. B can be standardized (Hurlbert 1978) and expressed as $B_{sta} = \frac{B-1}{n-1}$. The index was categorized as low (<0.4), moderate, (0.4—0.6), and high (>0.6) (Novakowski et al. 2008). We calculated spatial niche overlap between life stages using the symmetric measure proposed by Pianka (1973):

$$O_{ik} = \frac{\sum_i^n P_{ij}\ P_{ik}}{\sqrt{\sum_i^n P_{ij}^2 \sum_i^n P_{ik}^2}} \quad (4)$$

where O_{jk} is Pianka's measure of niche overlap between species j and species k; P_{ij} indicates that proportion resource i is of the total resources used by species j; P_{ik} indicates that proportion resource i is of the total resources used by species k; and n is total number of resource states. This symmetric measure of overlap functions so that overlap between species A and species B is identical to overlap between species B and species A, with values ranging from 0 (no overlap) to 1 (complete overlap). To provide a more nuanced interpretation of the overlap, the values were classified into 3 categories: low (0—0.39), intermediate (0.4—0.6), and high (0.61—1) (Grossman & Hart 1986).

The adequacy of stomach sample size for dietary analysis was assessed through a randomization approach. We plotted the relationship between the number of stomachs analyzed and the cumulative trophic diversity using the Shannon diversity index H. For robust statistical analysis, we performed 1000 randomizations of stomach content sequences for each sample group. From these iterations, we generated mean diversity curves. Sample sufficiency was determined when the diversity values stabilized—specifically, when at least 2 consecutive measurements before the final diversity value (H) fell within a ±5% range of the trophic diversity of the total sample (Alonso et al. 2002).

Stable isotopes and THg profiles were first compared among ontogenetic stage by conducting ANCOVA or Kruskal-Wallis tests including additional factors to account for the effects of sex and TL. Prior to conducting ANCOVA on $\delta^{13}C$, $\delta^{15}N$, and THg values across life stages, the assumptions of normality and homogeneity of variances were tested. Normality was assessed using the Shapiro-Wilk test, and homogeneity of variances was evaluated using Levene's test. When a significant effect was detected, Tukey post hoc tests with Kramer correction or post hoc Dunn tests with Bonferroni correction were performed to identify significant differences between factor levels, e.g. actual differences among ontogenetic stage. We then calculated the standard ellipse areas corrected for small sample size (SEAc) to quantify isotope niche space using the 'SIBER' package (Jackson et al. 2011, Skinner et al. 2019). The niche overlap between ontogenetic groups was estimated by determining the percentage of niche area of group 'A' (e.g. juvenile) that overlaps with group 'B' (e.g. subadult) to return a probability at 95% that group 'A' will overlap with group 'B'. The median overlap between 2 groups was 'high' if the estimated pairwise niche overlap was greater than 50%. The overlap calculations were performed using the 'nicheROVER' package (Swanson et al. 2015) in R version 4.3.2 (R Core Team 2023).

The relative isotopic contribution of prey to the diet was estimated using the Bayesian isotopic mixing model MixSIAR version 3.1.12 (Phillips et al. 2014). Because the number of isotopic tracers limits the number of prey items that can be included in the model, a hierarchical clustering analysis (Ward's linkage, Euclidean distance) was conducted using the mean $\delta^{13}C$ and $\delta^{15}N$ values of prey species to define functional groups. According to Layman et al. (2007), $\delta^{13}C$ and $\delta^{15}N$ ratios reflect the trophic signature of an organism within an ecosystem, and species exhibiting similar isotopic profiles are assumed to occupy similar trophic niches and fulfil comparable functional roles. Prior to analysis, data normality and homogeneity of variances were confirmed using Shapiro-Wilk and Levene's tests, respectively. One-way ANOVA was then applied to examine isotopic variability among the identified groups, followed by Tukey's post hoc test. The hierarchical clustering of isotopic ratios revealed 3 distinct functional groups (F_groups), which differed significantly in $\delta^{15}N$ values (ANOVA, $F_{3,26} = 459.2$, $p < 0.001$): 'F_group1' comprised 1 mesopelagic fish, 2 demersal fish, and 2 cephalopods; 'F_group2' consisted exclusively of decapods, and 'F_group3' was composed of 4 mesopelagic fish and 2 demersal fish. The model was run with 300 000 Markov chain Monte Carlo simulations (200 000 burn-in) and the convergence was evaluated using Gelman-Rubin (out of 116 variables: 0 > 1.05) and Geweke diagnostics (Geweke 1991, Gelman et al. 2013). For the mixing model, the $\delta^{13}C$ and $\delta^{15}N$ values were adjusted to a trophic level using the trophic discrimination factor estimates for muscle and liver from Hussey et al. (2010). All analyses were conducted in R version 4.3.2 (R Core Team 2023), with a significance level of $\alpha = 0.05$.

3. RESULTS

3.1. Diet preferences and ontogenetic feeding shift

Of the 285 *Etmopterus molleri* individuals examined, 115 (68 females and 47 males, including 40 juveniles, 45 subadults, and 30 adults) had consumed prey, indicating a 59.65% vacuity rate for the species. The sample size was sufficient for each life stage, with cumulative trophic diversity leveling out at 20–30 stomachs for juveniles, 40–50 for subadults, and 35–45 for adults (Fig. S1 in the Supplement at www.int-res.com/articles/suppl/m771p089_supp.pdf). Individual sharks exhibited a length range of 130.5–170.5 mm for juveniles, 196.6–268.7 mm for subadults, and 273.2–338.7 mm for adults. A total of 197 prey items from 16 taxa was found in the stomachs. Across all life stages, euphausiids were the dominant prey group (%PSIRI = 33.11), followed by decapods (%PSIRI = 30.16) and teleosts (%PSIRI = 26.15), while cephalopods represented sporadic prey items (%PSIRI = 10.54). A 1-way ANOSIM based on Euclidean distances revealed significant differences in diet composition across ontogenetic stages ($R = 0.085$, $p < 0.05$, 9999 permutations), but not between sexes ($R = -0.005$, $p = 0.63$, 9999 permutations). Pairwise comparisons showed significant differences between juveniles and other life stages, but not between adults and subadults ($p = 0.82$). Juveniles fed mainly on Pseudeuphausia sinica and *Euphausia nana* (%PSIRI = 51.40); subadults ate teleost fish (mainly *Diaphus* spp. and *Polymetme elongata*, %PSIRI = 41.20) and decapods (mainly *Heterocarpus* spp. and unidentified decapods, %PSIRI = 33.89); and adults ate predominately teleosts, decapods, and cephalopods (%PSIRI = 40.44, 30.85, and 28.76, respectively) (Table 1).

Certain species and groups contributed most to the dietary differences among *E. molleri* life stages. *P. sinica* was the predominant prey for juveniles, contributing over 60% to their diet, but its importance decreased dramatically in other life stages. *E. nana* played a significant role in the diets of both juveniles and subadults. Fish species, such as unidentified Teleostei, *P. elongata*, and *Diaphus* spp., showed more homogeneous contributions across adult and subadult life stages. Deepwater shrimp were particularly important in subadult diets (Table 2).

3.2. SIA and THg profiles

$\delta^{13}C$ and $\delta^{15}N$ values increased significantly across life stages in both muscle and liver tissues. For $\delta^{13}C$ in muscle tissue, ANCOVA revealed a significant effect of life stages (ANCOVA: $F_{2,77} = 31.02$, $p < 0.001$). Post hoc Tukey HSD tests showed that $\delta^{13}C$ values were significantly lower in juveniles compared to both adult and subadult life stages ($p < 0.001$), while the difference between subadults and adults was marginally significant ($p = 0.07$). In liver tissue, $\delta^{13}C$ also varied significantly among life stages ($F_{2,28} = 35.03$, $p < 0.001$), with significant differences between juveniles and both adult and subadult life stages ($p < 0.001$), but not between adults and subadults ($p = 0.20$). In contrast, $\delta^{15}N$ values differed significantly between juveniles and the other stages in both liver ($F_{2,28} = 33.83$, $p < 0.001$) and muscle ($F_{2,77} = 39.10$, $p < 0.001$) tissues, while no significant difference was observed between adults and subadults ($p = 0.79$).

Table 1. Diet composition of *Etmopterus molleri* between life stages in the East China Sea. %PN*i*: percentage in number; %PW*i*: percentage in weight; %FO*i*: frequency of occurrence; %PSIRI: prey-specific index of relative importance

	Juvenile				Subadult				Adult			
Prey groups	%PN	%PW	%FO	%PSIRI	%PN	%PW	%FO	%PSIRI	%PN	%PW	%FO	%PSIRI
Euphausiacea												
Pseudeuphausia sinica	84.61	85.9	37.14	31.67								
Euphausia nana	83.3	70.2	25.71	19.74	72.22	62.17	10	6.72				
Unidentified	72.2	68.1	25.71	18.04	70.83	69.37	13.33	9.35				
Decapoda												
Oplophorus spp.	88.8	94.4	8.57	7.85	55.56	58.07	10.00	5.68				
Pasiphaeidae spp.	100	100	2.86	2.86	66.67	58.7	10.00	6.27				
Acanthephyra armata	100	100	2.86	2.86	61.11	67.45	10.00	6.43	50	23.42	13.04	4.79
Plesionika spp.					66.67	54.41	3.33	2.02	87.5	68.38	8.70	6.78
Heterocarpus spp.	77.7	81.1	8.57	6.81	44.44	23.8	20.00	6.82	77.78	70.24	13.04	9.65
Unidentified	66.6	76.58	8.57	6.14	100	100	6.67	6.67	77.78	69.95	13.04	9.63
Cephalopoda												
Histioteuthis pacifica									100	100	4.35	4.35
Bathyteuthis abyssicola					41.67	31.67	6.67	2.44	100	100	13.04	13.04
Octopoteuthis spp.					50	31.43	3.33	1.36	100	100	8.70	8.70
Unidentified					66.67	85.06	6.67	5.06	66.67	56.28	4.35	2.67
Teleostei												
Diaphus spp.					47.22	66.51	20.00	11.37	83.33	84.58	8.70	7.30
Polymetme elongata					52.78	70.3	10.00	6.15	83.33	80.28	8.70	7.11
Neoscopelus microchir					83.33	86.21	6.67	5.65	100	100	4.35	4.35
Polyipnus spp.					55.56	65.42	10.00	6.05	33.33	41.58	8.70	3.26
Myctophidae spp.	50.00	89.95	5.71	4.00	66.67	89.76	6.67	5.21	41.67	61.21	13.04	6.71
Synagrops japonicus					50	24.29	6.67	2.48				
Unidentified					47.22	38.35	10.00	4.28	54.67	79.97	17.39	11.71

Table 2. SIMPER analysis of the prey found in *Etmopterus molleri*, stratified by life stage groups (juvenile, subadult, adult). Abundance: species contribution to average between-group dissimilarity; Avg. Diss: average dissimilarity; Cum%: cumulative percent

	Abundance (%)	Avg. Diss (%)	Cum%	p
Juvenile_Subadult				
Pseudeuphausia sinica	77.14	15.60 ± 21.70	16.6	0.01
Euphausia nana	48.57	12.15 ± 18.71	29.4	0.03
Synagrops japonicus	0	1.92 ± 7.7	96.3	0.2
Juvenile_Adult				
Pseudeuphausia sinica	77.14	16.24 ± 22.92	16.8	0.01
Histioteuthis pacifica	0	2.07 ± 9.85	92.7	0.05
Subadult_Adult				
Diaphus spp.	13.33	6.39 ± 11.89	26.90	0.03
Teleostei			40.80	0.01
Polymetme elongata	16.67	6.11 ± 14.16	47.40	0.01
Plesionika spp.	6.67	5.50 ± 15.45	53.30	0.04
Bathyteuthis abyssicola	6.67	3.80 ± 8.50	77.5	0.01

The $\delta^{13}C$ values varied between −18.95 and −16.91‰ for muscle tissue, with an average of −18.30‰ (−18.95 to −17.65‰) for juveniles, −17.62‰ (−18.46 to −16.92‰) for subadults, and −17.40‰ (−18.23 to −16.91‰) for adults. For liver tissue, $\delta^{13}C$ values ranged from −19.18 to −16.46‰, with an average of −18.74‰ (−19.18 to −17.67‰) for juveniles, −17.57‰ (−18.25 to −17.08‰) for subadults, and −17.22‰ (−18.05 to −16.46‰) for adults. The $\delta^{15}N$ values ranged between 9.91 and 13.56‰ for muscle, with an average of 10.83‰ (9.92–11.56‰) for juveniles, 12.02‰ (10.10–13.16‰) for subadults, and 12.52‰ (11.53–13.56‰) for adults. For liver tissue, $\delta^{15}N$ values varied between 9.16 and 12.32‰, with an average of 10.06‰ (9.16–10.84‰) for juveniles, 11.44‰ (10.82–12.07‰) for subadults, and 11.65‰ (10.88–12.32‰) for adults (Table 3). The potential prey species covered an overall isotopic space ranging from −19.95 ± 0.42 to −16.74 ± 0.01‰ in $\delta^{13}C$, and 7.48 ± 1.34 to 12.91 ± 0.09‰ in $\delta^{15}N$. The classification of the various potential prey into functional groups is summarized in Table S1.

THg concentrations increased with life stage (using size as a proxy for stage), particularly in muscle tissues, whereas juvenile and subadult stages exhibited

Table 3. Isotopic values (mean ± SD), total mercury values (THg, mean ± SD), and estimated trophic position (TP) for *Etmopterus molleri* across life stages, with sample sizes (N) shown separately for females (F) and males (M) and their main prey groups (see Section 2.5 for definitions) from the East China Sea

Tissue	Life stage	N (F/M)	$\delta^{13}C$ (‰)	$\delta^{15}N$ (‰)	THg (μg g^{-1} dry wt)	TP
Muscle	Juvenile	10/5	−18.30 ± 0.37	10.83 ± 0.42	0.60 ± 0.20	2.78
	Subadult	28/15	−17.62 ± 0.35	12.02 ± 0.68	1.95 ± 1.07	3.14
	Adult	11/10	−17.40 ± 0.33	12.52 ± 0.55	5.34 ± 2.82	3.31
Liver	Juvenile	5/5	−18.74 ± 0.46	10.06 ± 0.55	2.46 ± 1.96	
	Subadult	5/3	−17.57 ± 0.47	11.44 ± 0.39	2.04 ± 0.51	
	Adult	7/6	−17.22 ± 0.41	11.65 ± 0.47	3.43 ± 1.89	
Muscle (prey)	F_group1	20	−17.61 ± 0.39	11.98 ± 0.88	0.83 ± 0.37	
	F_group2	14	−19.29±0.57	7.75±0.61	0.04 ± 0.03	
	F_group3	35	−19.10 ± 0.34	10.23 ± 0.78	0.57 ± 0.23	

similar mean concentrations in liver tissues (Table 3). Adult life stages exhibited the highest mean concentrations (5.34 ± 2.82 and 3.43 ± 1.89 μg g^{-1} dry wt for muscle and liver, respectively). In muscle tissue, a Kruskal-Wallis test revealed a significant difference in THg concentrations across life stages (χ^2 = 42.51, df = 2, $p < 0.001$), with post hoc Dunn-Bonferroni comparisons indicating significantly higher concentrations in adults compared to subadults ($p = 0.0012$) and juveniles ($p < 0.001$), and in subadults compared to juveniles ($p < 0.001$). In liver tissue, no significant difference was detected between life stages (Kruskal-Wallis test: χ^2 = 2.82, df = 2, $p = 0.24$), and Dunn-Bonferroni pairwise comparisons confirmed the absence of significant differences ($p > 0.46$ in all cases). In juveniles, mean concentrations were significantly higher in liver compared to muscle tissue (Kruskal-Wallis χ^2 = 19.3, df = 2, $p < 0.05$), while subadults showed similar mean values across both tissues. Positive and significant correlations ($p < 0.05$) were observed between THg concentrations and all examined variables (i.e. TL, $\delta^{13}C$, and $\delta^{15}N$) (Fig. S2).

3.3. Niche estimation and overlap

Based on the SCA results, Levins' standardized niche breadth (B_{sta}) value for the entire sample was 0.83. However, clear differences were observed between life stages: juveniles exhibited a low diet breadth (B_{sta} = 0.31), reflecting a specialist feeding strategy, whereas subadults and adults displayed a more generalist strategy, characterized by B_{sta} values ⩾0.60. Additionally, Pianka's index of diet overlap revealed a high overlap between subadults and adults (0.90), an intermediate overlap between subadults and juveniles (0.52), and low dietary overlap between adults and juveniles (0.26) (Table 4).

Table 4. Pianka's diet overlap and Levins' niche breadth by life stage for *Etmopterus molleri* based on stomach content analysis. **Bold** values represent the significance indices

Life stage	Juvenile	Subadult	Adult
Juvenile		0.52	0.26
Subadult			**0.90**
Adult			
Levins niche (B_{sta})	0.31	**0.72**	**0.60**

SEAc using $\delta^{13}C$ and $\delta^{15}N$ revealed different sized niches among life stages, but with relatively similar breadth (Fig. 2). Subadults and adults presented a similar isotopic niche space (SEAc = 0.56‰^{2}), while juveniles displayed a smaller niche space (SEAc = 0.52‰^{2}).

When considering isotopic niche space, the niche overlap probabilities calculated with 95% credibility showed very low overlap between juveniles and adults (5.35%) and modest overlap with subadults

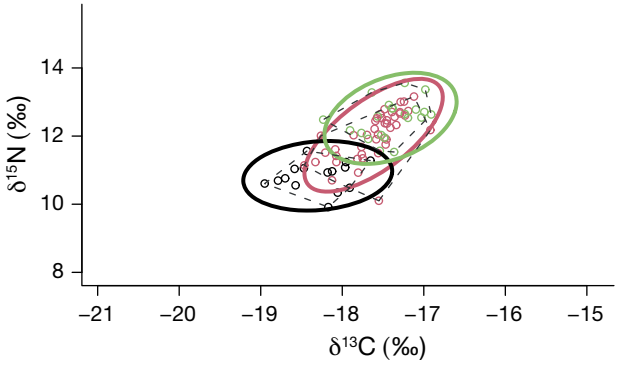

Fig. 2. Muscle $\delta^{13}C$ and $\delta^{15}N$ values of *Etmopterus molleri*. Dots represent different life stages: black — juvenile, red — subadult, green — adult. Solid lines delimit the standard ellipse areas (SEA) at 95% and dashed lines show the convex hull areas for each life stage

(27.95%), while subadults displayed high overlap with adults (86.45%) (Table 5, Fig. 3).

3.4. Stable isotope mixing model and prey contributions

MIXSIAR model results indicated ontogenetic variation in isotopic contributions among functional groups. In juveniles, F_group2 dominated both muscle (70.2%) and liver (70.1%) tissues, followed by F_group3 (22.6 and 23.7%, respectively). In subadults, contributions of F_group1 and F_group2 were relatively balanced across tissues (muscle: 41.1 and 52.8%; liver: 38.9 and 54.5%). In adults, prey contributions differed by tissue, with F_group1 and F_group2 comprising 51.6 and 40.6% in muscle and 58.5 and 39.6% in liver, respectively (Fig. S3).

Table 5. Probabilities (%) that an individual from life stage 'A' of *Etmopterus molleri* is found in the niche region of life stage 'B', calculated with the 'nicheROVER' package in R (Swanson et al. 2015) using $\delta^{13}C$ and $\delta^{15}N$. **Bold** values represent high overlap

	Life stage 'B'		
Life stage 'A'	Juvenile	Subadult	Adult
Juvenile		**50.41**	7.68
Subadult	27.95		**79.41**
Adult	5.35	**86.45**	

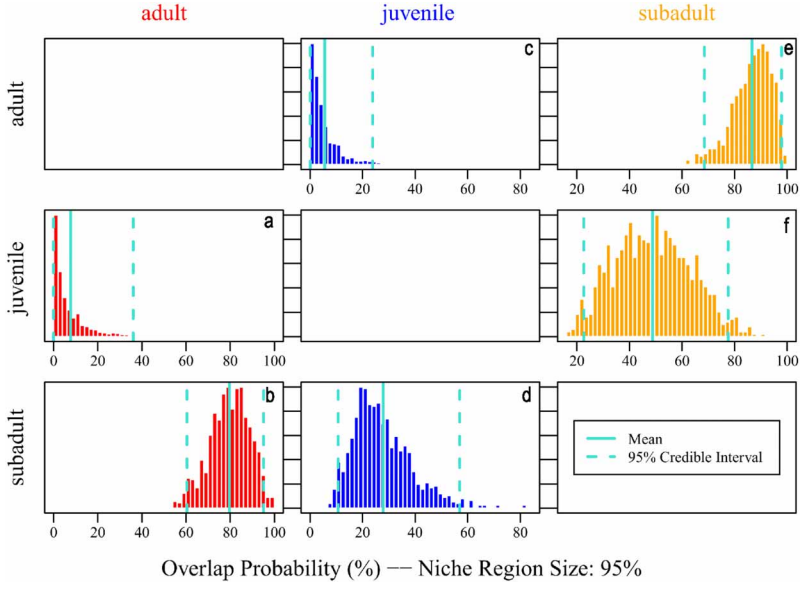

Fig. 3. Posterior distribution of the probabilistic niche overlap metric (%) for a specified niche region of 95% showing probability of overlap between ontogenetic stages of *Etmopterus molleri*. Adult probabilistic niche overlap metric between (a) juvenile life stage and (b) subadult life stage; juvenile probabilistic niche overlap metric between (c) adult life stage and (d) subadult life stage; and subadult probabilistic niche overlap metric between (e) adult life stage and (f) juvenile life stage. The posterior means and 95% credible intervals are displayed in turquoise

4. DISCUSSION

The lack of knowledge on the ecology of deepwater sharks reflects the general lack of research in deepwater habitats. The dietary composition of deepwater sharks represents a crucial aspect of understanding marine ecosystem dynamics and predator–prey interactions. The results of this study provide the first information on the trophic ecology of *Etmopterus molleri*, one of the smallest and least studied deepwater sharks, through SCA, SIA, and THg.

E. molleri displays complex feeding preferences with diets mainly composed of euphausiids, teleosts, and decapods. These sharks exhibit ontogenetic shifts in prey selection from juvenile to subadult and adult life stages. Previous SCA in another deepwater shark in the family Etmopteridae indicated similar prey trends to our findings, with some variations in prey dominance. Hallett & Daley (2011) reported that the main items in the stomachs of *E. unicolor* in the southeastern Pacific Ocean were benthic cephalopods, whereas benthic teleosts were dominant prey in the diet of *E. baxteri*. Dolganov (2019) reported myctophids, squids, and crustaceans as the main prey for *E. villosus* in the Pacific Ocean, while Xavier et al. (2012) reported fish and crustaceans as the main prey of *E. pusillus* in the northeast Atlantic Ocean.

The primary prey items of juvenile *E. molleri* were similar to those reported for juveniles of another congener, *E. spinax*, in the Western Mediterranean. In both species, euphausiids composed the main prey group for juveniles (Neiva et al. 2006), while crustaceans and teleosts constituted the primary prey for larger individuals. Adults and subadults exhibited diets characterized by an increased reliance on mesopelagic teleosts, decapods, and cephalopods; this result is in line with SCA results of larger individuals of *E. spinax* in the Western Mediterranean (Fanelli et al. 2009, Valls et al. 2017, Barría et al. 2018). For subadults, this transition can reflect a degree of opportunistic feeding behavior, likely

facilitated by their growing size, enhanced swimming capabilities, and improved hunting efficiency (Bornatowski et al. 2014, D'Iglio et al. 2021, Besnard et al. 2022). Interestingly, adult and subadult diets showed no significant differences, suggesting a plateau in dietary specialization with growth, although cephalopods remained secondary prey for adults. This finding is consistent with ecological theories suggesting that adult stages of predatory animals often have stable food preferences because they have developed optimal foraging strategies within their ecological niches (Wetherbee & Cortés 2004). The diet of *E. molleri* juveniles suggests that specialist feeding behavior may minimize competition with larger conspecifics and other sympatric predators, ensuring resource partitioning and enhancing survival during early development (Heupel & Simpfendorfer 2008, Ferretti et al. 2010, Xavier et al. 2012).

The observed diet composition of *E. molleri* across ontogenetic stages reveals a strong reliance on prey taxa commonly reported as bycatch in regional bottom trawl fisheries (Li et al. 2009, Naimullah et al. 2022, Sun et al. 2023). This trophic dependence on bentho-pelagic organisms associated with trawl-targeted habitats may increase the species' exposure to fishing pressure, particularly in intensively exploited areas (Zhang et al. 2016, Das et al. 2022, Graça et al. 2025). Subadults, which predominantly feed on decapods, may be indirectly affected by reductions in prey availability due to non-selective harvesting, whereas adults, which shift to larger prey such as teleosts and cephalopods, may face direct competition with commercial fisheries. Combined with their intrinsic life-history traits — slow growth, late sexual maturity, and low fecundity (Mboglen et al. 2025) — these observations emphasize the potential vulnerability of *E. molleri* to bottom trawl fisheries due to overlapping habitat use.

The SIA encompassed most of the species' life cycle; however, we excluded young of the year individuals due to the potential influence of maternal isotopic composition on this life stage (Olin et al. 2011, Malpica-Cruz et al. 2012, Rosende-Pereiro et al. 2020). Body size was linked to enrichment in $\delta^{13}C$ and $\delta^{15}N$ shifts through ontogenetic trophic changes, with variability decreasing with increasing TL. This finding is consistent with the general understanding that many elasmobranch species exhibit ontogenetic shifts in diet and habitat, which can be reflected in their stable isotope signatures (McMeans et al. 2010, Sánchez-Hernández et al. 2019, Priester et al. 2024). The significant differences in $\delta^{13}C$ and $\delta^{15}N$ values between juveniles and both adult and subadult groups, with no difference between adults and subadults, suggest that juveniles occupy a distinct habitat or display a specialist diet (Hussey et al. 2011, Sogawa et al. 2017, Zhou et al. 2021). Subadults and adults exhibited higher $\delta^{15}N$ values, reflecting a dietary shift to prey enriched in $\delta^{15}N$ as confirmed by SCA. This observation concords with previous studies on other predators, where ontogenetic increases in $\delta^{15}N$ values were attributed to the consumption of prey from higher trophic levels (Hussey et al. 2010, Vaudo & Heithaus 2011, Matich et al. 2019). The subadult group exhibited a wider $\delta^{15}N$ range compared with the adult group, suggesting that subadults occupy diverse habitats across depth ranges and display a broad trophic niche. Trophic position in marine organisms is closely linked to habitat use and depth, particularly in deepwater ecosystems where vertical environmental gradients strongly influence food web structure (Drazen & Sutton 2017). Research has shown that depth stratification results in distinct isotopic signatures ($\delta^{13}C$ and $\delta^{15}N$), reflecting changes in resource availability and trophic interactions across depth (Cartes & Carrassón 2004, Houssard et al. 2017). Thus, juveniles typically inhabit shallower and more productive environments, resulting in lower $\delta^{15}N$ values due to feeding at lower trophic levels. As they grow and migrate to deeper waters, subadults gain access to prey from higher trophic levels, leading to a broader $\delta^{15}N$ range compared to adults, who have already reached a trophic plateau in terms of prey composition. As an active deepwater predator, the slendertail lanternshark possesses swimming capabilities enabling it to reach shallower waters (Pinte et al. 2020). This mobility allows the species to exploit both epipelagic prey that perform diel vertical migrations and demersal prey, which explains the diversity of prey items observed in its diet.

Overall, the mixing models suggested that *E. molleri* feeds on a broad prey spectrum representing multiple functional groups as defined by hierarchical classification. Although the prey selected for the models were not exhaustive, they encompassed the main species documented in the literature as potential prey for deepwater sharks. Mesopelagic teleosts and crustaceans contributed most significantly to the diet of subadult and juvenile life stages, respectively, while adults showed a preference for demersal teleosts and cephalopods. Graça Aranha et al. (2023) reported that cephalopods and crustaceans were the main prey contribution for *E. pusillus* based on SIA. Isotopic prey contributions were similar between analyzed tissues, especially for juveniles. The relative contributions of different prey categories were consistent between liver and muscle tissues in juveniles, accord-

ing to $\delta^{13}C$ and $\delta^{15}N$ signatures. This consistency suggests stable feeding habits and limited diet shifts over time, likely reflecting the occupation of homogeneous habitats with relatively constant resource availability during early life stages. Similar patterns have been reported in other sharks, where early developmental phases are associated with restricted habitat ranges and specialized foraging strategies (Hussey et al. 2011, Matich et al. 2015). The observed differences in prey isotopic contribution to the diet of adult and subadult individuals may indicate seasonal dietary shifts; further studies should be conducted to confirm this observation. The estimated probabilities of trophic niche overlap between life stages can serve as indicators of resource segregation throughout the life cycle. The low overlap of niches between life stages reveals adaptive dietary preferences that help avoid trophic competition and ensure population stability (Priester et al. 2024). Differences in diet preference corroborate this isotopic interpretation, which applies to our results. Overall, the progressive expansion of isotopic niche space and the increase in $\delta^{15}N$ values with size suggest a transition from a specialist feeding regime to a more opportunistic diet during growth.

The amplitude and overlap of trophic niches derived from dietary analyses (SCA and SIA) are consistent with the observed ontogenetic shifts. The slendertail lanternshark displayed feeding pattern transitions from a specialist strategy in juveniles, focusing primarily on euphausiid prey, to an opportunistic/generalist approach in larger individuals. This ontogenetic broadening of trophic niche has been widely documented among deepwater sharks (Lucifora et al. 2009, Newman et al. 2012). Similar ontogenetic shifts have been reported in several squaliform sharks, including *E. spinax* (Neiva et al. 2006), *Centrophorus squamosus* (Preciado et al. 2009), and *Squalus megalops* (Braccini et al. 2005). The transition from crustacean-dominated to fish-dominated diets may also represent an optimization strategy, as teleosts generally provide higher energy returns per unit of foraging effort compared to crustacean prey (Ferretti et al. 2018). Furthermore, these dietary shifts could serve to reduce intraspecific competition between life stages by partitioning food resources, a strategy commonly observed in size-structured populations of marine predators (Ebert 2002, Navarro et al. 2014).

Our results support previous findings indicating that mercury bioaccumulation in deep-sea organisms is tightly linked to trophic position and habitat use. The significant differences in $\delta^{13}C$ and $\delta^{15}N$ values observed between juveniles and older stages suggest ontogenetic shifts in habitat and diet, which are known to influence mercury uptake (Pethybridge et al. 2010, Zheng et al. 2019). In the juvenile life stage, the stable and low $\delta^{15}N$ values reflect feeding at lower trophic levels, likely in shallower habitats where mercury concentrations are comparatively lower. As individuals mature and migrate to deeper zones, they probably encounter prey with higher mercury loads, resulting in elevated tissue concentrations. This ontogenetic trajectory echoes patterns documented in mesopelagic ecosystems, where mercury accumulation is shaped by vertical habitat use and food web connectivity (Monteiro et al. 1996, Chouvelon et al. 2018, Li et al. 2023).

Combined with $\delta^{15}N$, THg can help determine how the trophic position of a consumer affects mercury accumulation in marine food webs (Chouvelon et al. 2011, Lavoie et al. 2013, Bezerra et al. 2021). In this study, *E. molleri* showed THg concentrations similar to other deepwater shark species globally, including those from Australia (Pethybridge et al. 2010, 2012), South Africa (Le Bourg et al. 2019), and the North Atlantic Ocean (Newman et al. 2011). However, these concentrations were significantly higher than those found in a congener, *E. spinax*, in the Mediterranean (Rodrigues et al. 2022). Overall, intraspecific variations in THg concentration could be explained by $\delta^{15}N$ and potential prey found in the stomach, as well as TL and depth selectivity. Higher $\delta^{15}N$ values, indicating a higher trophic level, are associated with increased mercury bioaccumulation due to biomagnification across the food web (Chouvelon et al. 2011, Lavoie et al. 2013). Additionally, larger individuals, as reflected by the TL, may accumulate more mercury over time through prolonged exposure and dietary intake. Variations in prey composition, revealed through SCA, further suggest that individuals feeding on higher trophic levels or more contaminated prey items are subjected to higher THg burdens. Importantly, habitat selectivity, particularly depth preference, may also play a significant role, as mercury concentrations in deep-sea environments are known to increase with depth due to methylation processes and sedimentation (Choy et al. 2009, Blum et al. 2013, Zhang et al. 2024). Thus, individuals exploiting deeper habitats may experience greater exposure to bioavailable mercury, compounding the effects of trophic position and prey type on THg accumulation.

Previous studies on other deepwater sharks have found similar results; Pethybridge et al. (2012) and Le Bourg et al. (2019) observed a significant correlation between log-transformed THg and $\delta^{15}N$ when individuals from different shark species were pooled. How-

ever, contrary trends (negative correlations) have been reported in pelagic sharks, such as the silky shark in the eastern tropical Pacific Ocean, which showed a depletion in $\delta^{15}N$ with increasing THg concentration and life stage (Li et al. 2022). This is probably because mature individuals move to pelagic waters, which may be linked to places where nitrogen is fixed, which lowers baseline $\delta^{15}N$ values (Pethybridge et al. 2018, Li et al. 2023). A comparable pattern was observed in the dermal tissue of silky and blue sharks from the northeast central Pacific, where larger individuals showed lower $\delta^{15}N$ values, likely associated with shifts in foraging habitats (Li et al. 2016).

5. CONCLUSIONS

Understanding the trophic ecology of deepwater sharks has long been hindered by the logistical challenges of sampling at depth. This study provides the first integrative assessment of the feeding ecology of *Etmopterus molleri*, a small and poorly known shark species inhabiting the ECS. Using SCA, stable isotope ratios, and THg concentrations, we document clear ontogenetic shifts in diet composition, trophic position, and niche breadth. Juveniles primarily consumed small pelagic crustaceans, while subadults and adults exploited a broader range of prey, including decapods, teleosts, and cephalopods, reflecting a progressive transition to higher trophic levels and greater diet diversity throughout the life cycle. These findings not only enhance our understanding of the ecological role of *E. molleri* but also highlight the need to consider dietary ecology in assessments of fishing impacts on deep-sea shark populations — especially for species like *E. molleri* that inhabit areas overlapping with bottom trawl operations and rely on prey frequently caught as bycatch.

Data availability. The raw data supporting the conclusions of this article will be made available by the authors, without undue reservation.

Acknowledgements. This work was supported by the National Natural Science Foundation of China (#42276092) and the Program for Professor of Special Appointment (Eastern Scholar) at Shanghai Institutions of Higher Learning. We thank the staff at Shanghai Ocean University for their assistance with sample collection and preparation. We followed all applicable institutional or national guidelines for the care and use of animals. All samples in this study were dead bycaught sharks that were not caught during illegal commercial activities. This scientific research activity complies with the relevant requirements of the Wildlife Protection Law of the People's Republic of China.

LITERATURE CITED

Alonso MK, Crespo EA, García NA, Pedraza SN, Mariotti PA, Mora NJ (2002) Fishery and ontogenetic driven changes in the diet of the spiny dogfish, *Squalus acanthias*, in Patagonian waters, Argentina. Environ Biol Fishes 63:193–202

Amundsen PA, Sánchez-Hernández J (2019) Feeding studies take guts — critical review and recommendations of methods for stomach contents analysis in fish. J Fish Biol 95:1364–1373

Bailey DM, Collins MA, Gordon JDM, Zuur AF, Priede IG (2009) Long-term changes in deep-water fish populations in the northeast Atlantic: a deeper reaching effect of fisheries? Proc R Soc B 276:1965–1969

Barría C, Navarro J, Coll M (2018) Feeding habits of four sympatric sharks in two deep-water fishery areas of the western Mediterranean Sea. Deep Sea Res I 142:34–43

Bergstad OA, Wik ÅD, Hildre Ø (2003) Predator-prey relationships and food sources of the Skagerrak deep-water fish assemblage. J Northwest Atl Fish Sci 31:165–180

Besnard L, Duchatelet L, Bird CS, Le Croizier G and others (2022) Diet consistency but large-scale isotopic variations in a deep-sea shark: the case of the velvet belly lantern shark, *Etmopterus spinax*, in the northeastern Atlantic region and Mediterranean Sea. Deep Sea Res I 182:103708

Bezerra MF, Seminoff JA, Lemons GE, Slotton DG, Watanabe K, Lai CT (2021) Trophic ecology of sympatric batoid species (Chondrichthyes: Batoidea) assessed by multiple biogeochemical tracers ($\delta^{13}C$, $\delta^{15}N$ and total Hg). Environ Res 199:111398

Bird CS, Veríssimo A, Magozzi S, Abrantes KG and others (2018) A global perspective on the trophic geography of sharks. Nat Ecol Evol 2:299–305

Blum JD, Popp BN, Drazen JC, Anela Choy C, Johnson MW (2013) Methylmercury production below the mixed layer in the North Pacific Ocean. Nat Geosci 6:879–884

Bornatowski H, Navia AF, Braga RR, Abilhoa V, Corrêa MFM (2014) Ecological importance of sharks and rays in a structural foodweb analysis in southern Brazil. ICES J Mar Sci 71:1586–1592

Braccini JM, Gillanders BM, Walker TI (2005) Sources of variation in the feeding ecology of the piked spurdog (*Squalus megalops*): implications for inferring predator–prey interactions from overall dietary composition. ICES J Mar Sci 62:1076–1094

Brown SC, Bizzarro J, Cailliet GM, Ebert DA (2012) Breaking with tradition: redefining measures for diet description with a case study of the Aleutian skate *Bathyraja aleutica* (Gilbert 1896). Environ Biol Fishes 95:3–20

Carlisle AB, Allan EA, Kim SL, Meyer L, Port J, Scherrer S, O'Sullivan J (2021) Integrating multiple chemical tracers to elucidate the diet and habitat of cookiecutter sharks. Sci Rep 11:11809

Cartes JE, Carrassón M (2004) Influence of trophic variables on the depth-range distributions and zonation rates of deep-sea megafauna: the case of the Western Mediterranean assemblages. Deep Sea Res I 51:263–279

Chouvelon T, Spitz J, Cherel Y, Caurant F, Sirmel R, Mèndez-Fernandez P, Bustamante P (2011) Inter-specific and ontogenic differences in $\delta^{13}C$ and $\delta^{15}N$ values and Hg and Cd concentrations in cephalopods. Mar Ecol Prog Ser 433:107–120

Chouvelon T, Cresson P, Bouchoucha M, Brach-Papa C and others (2018) Oligotrophy as a major driver of mercury

bioaccumulation in medium-to high-trophic level consumers: a marine ecosystem-comparative study. Environ Pollut 233:844–854

Choy CA, Popp BN, Kaneko JJ, Drazen JC (2009) The influence of depth on mercury levels in pelagic fishes and their prey. Proc Natl Acad Sci USA 106:13865–13869

Churchill DA, Heithaus MR, Vaudo JJ, Grubbs RD, Gastrich K, Castro JI (2015) Trophic interactions of common elasmobranchs in deep-sea communities of the Gulf of Mexico revealed through stable isotope and stomach content analysis. Deep Sea Res II 115:92–102

Colwell RK, Futuyma DJ (1971) On the measurement of niche breadth and overlap. Ecology 52:567–576

Cortés E (1999) Standardized diet compositions and trophic levels of sharks. ICES J Mar Sci 56:707–717

Dalerum F, Angerbjörn A (2005) Resolving temporal variation in vertebrate diets using naturally occurring stable isotopes. Oecologia 144:647–658

Daly R, Froneman PW, Smale MJ (2013) Comparative feeding ecology of bull sharks (*Carcharhinus leucas*) in the coastal waters of the southwest Indian Ocean inferred from stable isotope analysis. PLOS ONE 8:e78229

Das D, Gonzalez-Irusta JM, Morato T, Fauconnet L and others (2022) Distribution models of deep-sea elasmobranchs in the Azores, Mid-Atlantic Ridge, to inform spatial planning. Deep Sea Res I 182:103707

deVries MS, Del Rio CM, Tunstall TS, Dawson TE (2015) Isotopic incorporation rates and discrimination factors in mantis shrimp crustaceans. PLOS ONE 10:e0122334

D'Iglio C, Savoca S, Rinelli P, Spanò N, Capillo G (2021) Diet of the deep-sea shark *Galeus melastomus* Rafinesque, 1810, in the Mediterranean Sea: what we know and what we should know. Sustainability 13:3962

Dolganov VN (2019) On the little-known sharks *Etmopterus villosus* (Etmopteridae) and *Scymnodalatias sherwoodi* (Somniosidae) from the Pacific Ocean. J Ichthyol 59: 275–279

Drazen JC, Sutton TT (2017) Dining in the deep: the feeding ecology of deep-sea fishes. Annu Rev Mar Sci 9:337–366

Du J, Ding L, Su S, Hu W and others (2022) Setting conservation priorities for marine sharks in China and the Association of Southeast Asian Nations (ASEAN) Seas: What are the benefits of a 30% conservation target? Front Mar Sci 9:933291

Dulvy NK, Fowler SL, Musick JA, Cavanagh RD and others (2014) Extinction risk and conservation of the world's sharks and rays. eLife 3:e00590

Dulvy NK, Pacoureau N, Rigby CL, Pollom RA and others (2021) Overfishing drives over one-third of all sharks and rays toward a global extinction crisis. Curr Biol 31: 4773–4787

Ebert DA (2002) Ontogenetic changes in the diet of the sevengill shark (*Notorynchus cepedianus*). Mar Freshw Res 53:517–523

Ebert DA, Fowler S, Compagno L (2013) Sharks of the world: a fully illustrated guide. Wild Nature Press, Plymouth

Ebert DA, Leslie RW, Weigmann S (2021a) *Etmopterus brosei* sp. nov.: a new lanternshark (Squaliformes: Etmopteridae) from the southeastern Atlantic and southwestern Indian oceans, with a revised key to the *Etmopterus lucifer* clade. Mar Biol 51:53

Ebert DA, Dando M, Fowler S (2021b) Sharks of the world: a complete guide. Princeton University Press, Princeton, NJ

Fanelli E, Rey J, Torres P, Gil De Sola L (2009) Feeding habits of blackmouth catshark *Galeus melastomus* Rafinesque, 1810 and velvet belly lantern shark *Etmopterus spinax* (Linnaeus, 1758) in the western Mediterranean. J Appl Ichthyol 25:83–93

Feng JC, Liang J, Cai Y, Zhang S, Xue J, Yang Z (2022) Deep-sea organisms research oriented by deep-sea technologies development. Sci Bull 67:1802–1816

Ferretti F, Worm B, Britten GL, Heithaus MR, Lotze HK (2010) Patterns and ecosystem consequences of shark declines in the ocean. Ecol Lett 13:1055–1071

Ferretti F, Curnick D, Liu K, Romanov EV, Block BA (2018) Shark baselines and the conservation role of remote coral reef ecosystems. Sci Adv 4:eaaq0333

Finucci B, Pacoureau N, Rigby CL, Matsushiba JH and others (2024) Fishing for oil and meat drives irreversible defaunation of deepwater sharks and rays. Science 383: 1135–1141

Gelman A, Carlin JB, Stern HS, Dunson DB, Vehtari A, Rubin DB (2013) Bayesian data analysis. Chapman and Hall/CRC, London

Geweke J (1991) Evaluating the accuracy of sampling-based approaches to the calculation of posterior moments. Staff Report. Federal Reserve Bank of Minneapolis, Minneapolis, MN

Goyanna FAA, Fernandes MB, Silva GB, Lacerda LD (2023) Mercury in oceanic upper trophic level sharks and bony fishes - a systematic review. Environ Pollut 318:120821

Graça Aranha S, Teodósio A, Baptista V, Erzini K, Dias E (2023) A glimpse into the trophic ecology of deep-water sharks in an important crustacean fishing ground. J Fish Biol 102:655–668

Graça Aranha S, Dias E, Marsili T, Barkai A, Queiroz N, Pires da Rocha P, Teodósio A (2025) Unravelling the deep: assessing the bycatch of deep-sea elasmobranchs in crustacean bottom trawl fisheries in Portugal. Mar Pol 173: 106555

Grossman SJ, Hart OD (1986) The costs and benefits of ownership: a theory of vertical and lateral integration. J Polit Econ 94:691–719

Guo Z, Gon Y, Li Z, Shen Y, Li Y (2023) Lipid-extracted muscle and liver tissues: Can they reveal mercury exposure of pelagic sharks? Chemosphere 340:139873

Hallett CS, Daley RK (2011) Feeding ecology of the southern lanternshark (*Etmopterus baxteri*) and the brown lanternshark (*E. unicolor*) off southeastern Australia. ICES J Mar Sci 68:157–165

Heithaus MR (2004) Fish communities of subtropical seagrass meadows and associated habitats in Shark Bay, Western Australia. Bull Mar Sci 75:79–99

Heupel MR, Simpfendorfer CA (2008) Movement and distribution of young bull sharks *Carcharhinus leucas* in a variable estuarine environment. Aquat Biol 1:277–289

Heupel MR, Knip DM, Simpfendorfer CA, Dulvy NK (2014) Sizing up the ecological role of sharks as predators. Mar Ecol Prog Ser 495:291–298

Hewitt DE, Taylor MD, Raoult V, Smith TM, Gaston TF (2021) Diet-tissue discrimination and turnover of $\delta^{13}C$ and $\delta^{15}N$ in muscle tissue of a penaeid prawn. Rapid Commun Mass Spectrom 35:e9167

Hilgendag IR, Swanson HK, Lewis CW, Ehrman AD, Power M (2022) Mercury biomagnification in benthic, pelagic, and benthopelagic food webs in an Arctic marine ecosystem. Sci Total Environ 841:156424

Houssard P, Lorrain A, Tremblay-Boyer L, Allain V and others (2017) Trophic position increases with thermo-

cline depth in yellowfin and bigeye tuna across the Western and Central Pacific Ocean. Prog Oceanogr 154:49–63
Hurlbert HS (1978) The measurement of niche overlap and some relatives. Ecology 59:67–77
Hussey NE, Brush J, McCarthy ID, Fisk AT (2010) $\delta^{15}N$ and $\delta^{13}C$ diet-tissue discrimination factors for large sharks under semi-controlled conditions. Comp Biochem Physiol A Mol Integr Physiol 155:445–453
Hussey NE, Dudley SFJ, McCarthy ID, Cliff G, Fisk AT (2011) Stable isotope profiles of large marine predators: viable indicators of trophic position, diet, and movement in sharks? Can J Fish Aquat Sci 68:2029–2045
Hussey NE, MacNeil MA, Olin JA, McMeans BC, Kinney MJ, Chapman DD, Fisk AT (2012) Stable isotopes and elasmobranchs: tissue types, methods, applications and assumptions. J Fish Biol 80:1449–1484
Hussey NE, MacNeil MA, McMeans BC, Olin JA and others (2014) Rescaling the trophic structure of marine food webs. Ecol Lett 17:239–250
Hyodo F, Kohzu A, Tayasu I (2010) Linking aboveground and belowground food webs through carbon and nitrogen stable isotope analyses. Ecol Res 25:745–756
Hyslop EJ (1980) Stomach contents analysis — a review of methods and their application. J Fish Biol 17:411–429
Ishikawa NF, Hyodo F, Tayasu I (2013) Use of carbon-13 and carbon-14 natural abundances for stream food web studies. Ecol Res 28:759–769
Jackson AL, Inger R, Parnell AC, Bearhop S (2011) Comparing isotopic niche widths among and within communities: SIBER — Stable Isotope Bayesian Ellipses in R. J Anim Ecol 80:595–602
Jorgensen SJ, Micheli F, White TD, Van Houtan KS and others (2022) Emergent research and priorities for shark and ray conservation. Endang Species Res 47:171–203
Kim SL, Casper DR, Galván-Magaña F, Ochoa-Díaz R, Hernández-Aguilar SB, Koch PL (2012) Carbon and nitrogen discrimination factors for elasmobranch soft tissues based on a long-term controlled feeding study. Environ Biol Fishes 95:37–52
Kiszka JJ, Aubail A, Hussey NE, Heithaus MR, Caurant F, Bustamante P (2015) Plasticity of trophic interactions among sharks from the oceanic south-western Indian Ocean revealed by stable isotope and mercury analyses. Deep Sea Res I 96:49–58
Kolasinski J, Frouin P, Sallon A, Rogers K, Bruggemann HJ, Potier M (2009) Feeding ecology and ontogenetic dietary shift of yellowstripe goatfish *Mulloidichthys flavolineatus* (Mullidae) at Reunion Island, SW Indian ocean. Mar Ecol Prog Ser 386:181–195
Kousteni V (2021) Shedding light on the deep: the case of the velvet belly lanternshark in the North Aegean Sea. J Fish Biol 99:101–117
Kyne PM, Ebert DA, Schaaf-Da Silva A (2015) *Etmopterus molleri*. The IUCN Red List of Threatened Species 2015: e.T161407A68622705 (accessed 13 October 2024)
Lamborg CH, Hammerschmidt CR, Bowman KL, Swarr GJ and others (2014) A global ocean inventory of anthropogenic mercury based on water column measurements. Nature 512:65–68
Last PR, Stevens JD (2009) Sharks and rays of Australia, 2nd edn. CSIRO Publishing, Collingwood
Lavoie RA, Jardine TD, Chumchal MM, Kidd KA, Campbell LM (2013) Biomagnification of mercury in aquatic food webs: a worldwide meta-analysis. Environ Sci Technol 47: 13385–13394
Layman CA, Arrington DA, Montaña CG, Post DM (2007) Can stable isotope ratios provide for community-wide measures of trophic structure? Ecology 88:42–48
Le Bourg B, Kiszka JJ, Bustamante P, Heithaus MR, Jaquemet S, Humber F (2019) Effect of body length, trophic position and habitat use on mercury concentrations of sharks from contrasted ecosystems in the southwestern Indian Ocean. Environ Res 169:387–395
Le Croizier G, Lorrain A, Schaal G, Ketchum J and others (2020) Trophic resources and mercury exposure of two silvertip shark populations in the Northeast Pacific Ocean. Chemosphere 253:126645
Li Y, Zhang Y (2012) Fisheries impact on the East China Sea Shelf ecosystem for 1969-2000. Helgol Mar Res 66: 371–383
Li Y, Chen Y, Olson D, Yu N, Chen L (2009) Evaluating ecosystem structure and functioning of the East China sea shelf ecosystem, China. Hydrobiologia 636:331–351
Li Y, Zhang Y, Hussey NE, Dai X (2016) Urea and lipid extraction treatment effects on $\delta^{15}N$ and $\delta^{13}C$ values in pelagic sharks. Rapid Commun Mass Spectrom 30:1–8
Li Z, Pethybridge HR, Gong Y, Wu F, Dai X, Li Y (2022) Effect of body size, feeding ecology and maternal transfer on mercury accumulation of vulnerable silky shark *Carcharhinus falciformis* in the eastern tropical pacific. Environ Pollut 309:119751
Li Z, Pethybridge HR, Wu F, Li Y (2023) Mercury bioaccumulation in thresher sharks from the eastern tropical Pacific: influences of body size, maturation stage, and feeding habitat. Sci Total Environ 872:162248
Linnebjerg JF, Hobson KA, Fort J, Nielsen TG and others (2016) Deciphering the structure of the West Greenland marine food web using stable isotopes ($\delta^{13}C$, $\delta^{15}N$). Mar Biol 163:230
Logan JM, Lutcavage ME (2010) Stable isotope dynamics in elasmobranch fishes. Hydrobiologia 644:231–244
Lucifora LO, García VB, Escalante AH (2009) How can the feeding habits of the sand tiger shark influence the success of conservation programs? Anim Conserv 12: 291–301
Malpica-Cruz L, Herzka SZ, Sosa-Nishizaki O, Lazo JP (2012) Tissue-specific isotope trophic discrimination factors and turnover rates in a marine elasmobranch: empirical and modeling results. Can J Fish Aquat Sci 69:551–564
Manlick PJ, Newsome SD (2022) Stable isotope fingerprinting traces essential amino acid assimilation and multichannel feeding in a vertebrate consumer. Methods Ecol Evol 13:1819–1830
Matich P, Kiszka JJ, Heithaus MR, Mourier J, Planes S (2015) Short-term shifts of stable isotope ($\delta^{13}C$, $\delta^{15}N$) values in juvenile sharks within nursery areas suggest rapid shifts in energy pathways. J Exp Mar Biol Ecol 465: 83–91
Matich P, Kiszka JJ, Heithaus MR, Le Bourg B, Mourier J (2019) Inter-individual differences in ontogenetic trophic shifts among three marine predators. Oecologia 189: 621–636
Mboglen D, Gong Y, Guo Z, Ngo Nola D, Li Y (2024) First report of plastic and non-plastic microparticles in stomach of slendertail lanternshark and shortspine spurdog from the edge of East China Sea. Mar Pollut Bull 204: 116531
Mboglen D, Ebango Ngando N, Yongfu S, Li Y (2025) Deciphering age, growth, and maturity patterns in one of the smallest but data-deficient shark species, slendertail lan-

ternshark (*Etmopterus molleri*) from the East China Sea. J Fish Biol 107:788–807

McMeans BC, Svavarsson J, Dennard S, Fisk AT (2010) Diet and resource use among Greenland sharks (*Somniosus microcephalus*) and teleosts sampled in Icelandic waters, using $\delta^{13}C$, $\delta^{15}N$, and mercury. Can J Fish Aquat Sci 67: 1428–1438

Monteiro LR, Costa V, Furness RW, Santos RS (1996) Mercury concentrations in prey fish indicate enhanced bioaccumulation in mesopelagic environments. Mar Ecol Prog Ser 141:21–25

Naimullah M, Lee WY, Wu YL, Chen YK, Huang YC, Liao CH, Lan KW (2022) Effect of soaking time on targets and bycatch species catch rates in fish and crab trap fishery in the southern East China Sea. Fish Res 250:106258

Navarro J, López L, Coll M, Barría C, Sáez-Liante R (2014) Short- and long-term importance of small sharks in the diet of the rare deep-sea shark *Dalatias licha*. Mar Biol 161:1697–1707

Neiva J, Coelho R, Erzini K (2006) Feeding habits of the velvet belly lanternshark *Etmopterus spinax* (Chondrichthyes: Etmopteridae) off the Algarve, southern Portugal. J Mar Biol Assoc UK 86:835–841

Newman MC, Xu X, Cotton CF, Tom KR (2011) High mercury concentrations reflect trophic ecology of three deep-water chondrichthyans. Arch Environ Contam Toxicol 60:618–625

Newman SP, Handy RD, Gruber SH (2012) Ontogenetic diet shifts and prey selection in nursery bound lemon sharks, *Negaprion brevirostris*, indicate a flexible foraging tactic. Environ Biol Fishes 95:115–126

Norse EA, Brooke S, Cheung WWL, Clark MR and others (2012) Sustainability of deep-sea fisheries. Mar Policy 36: 307–320

Novakowski GC, Hahn NS, Fugi R (2008) Diet seasonality and food overlap of the fish assemblage in a pantanal pond. Neotrop Ichthyol 6:567–576

Ohshimo S, Tanaka H, Nishiuchi K, Yasuda T (2016) Trophic positions and predator–prey mass ratio of the pelagic food web in the East China Sea and Sea of Japan. Mar Freshw Res 67:1692–1699

Olin JA, Hussey NE, Fritts M, Heupel MR, Simpfendorfer CA, Poulakis GR, Fisk AT (2011) Maternal meddling in neonatal sharks: implications for interpreting stable isotopes in young animals. Rapid Commun Mass Spectrom 25:1008–1016

Pethybridge H, Cossa D, Butler ECV (2010) Mercury in 16 demersal sharks from southeast Australia: biotic and abiotic sources of variation and consumer health implications. Mar Environ Res 69:18–26

Pethybridge H, Butler ECV, Cossa D, Daley R, Boudou A (2012) Trophic structure and biomagnification of mercury in an assemblage of deepwater chondrichthyans from southeastern Australia. Mar Ecol Prog Ser 451: 163–174

Pethybridge HR, Choy CA, Polovina JJ, Fulton EA (2018) Improving marine ecosystem models with biochemical tracers. Annu Rev Mar Sci 10:199–228

Phillips DL, Inger R, Bearhop S, Jackson AL and others (2014) Best practices for use of stable isotope mixing models in food-web studies. Can J Zool 92:823–835

Pianka ER (1973) The structure of lizard communities. Annu Rev Ecol Syst 4:53–74

Pinte N, Parisot P, Martin U, Zintzen V, De Vleeschouwer C, Roberts CD, Mallefet J (2020) Ecological features and swimming capabilities of deep-sea sharks from New Zealand. Deep Sea Res I 156:103187

Post DM (2002) Using stable isotopes to estimate trophic position: models, methods, and assumptions. Ecology 83: 703–718

Preciado I, Cartes JE, Serrano A, Velasco F, Olaso I, Sánchez F, Frutos I (2009) Resource utilization by deep-sea sharks at the le Danois Bank, Cantabrian Sea, north-east Atlantic Ocean. J Fish Biol 75:1331–1355

Priester CR, Dierking J, Hansen T, Abecasis D, Fontes JM, Afonso P (2024) Trophic ecology and coastal niche partitioning of two sympatric shark species in the Azores (mid-Atlantic). Mar Ecol Prog Ser 726:113–130

R Core Team (2023) R: a language and environment for statistical computing. R Foundation for Statistical Computing, Vienna. https://www.R-project.org/

Reum JCP, Williams GD, Harvey CJ (2017) Stable isotope applications for understanding shark ecology in the northeast Pacific Ocean. Adv Mar Biol 77:149–178

Reum JCP, Williams GD, Harvey CJ, Andrews KS, Levin PS (2020) Trophic ecology of a large-bodied marine predator, bluntnose sixgill shark *Hexanchus griseus*, inferred using stable isotope analysis. Environ Biol Fishes 103: 147–162

Riesgo L, Sanpera C, García-Barcelona S, Sánchez-Fortún M, Coll M, Navarro J (2023) Understanding the role of ecological factors affecting mercury concentrations in the blue shark (*Prionace glauca*). Chemosphere 313: 137642

Rodrigues ACM, Gravato C, Galvão D, Silva VS and others (2022) Ecophysiological effects of mercury bioaccumulation and biochemical stress in the deep-water mesopredator *Etmopterus spinax* (Elasmobranchii; Etmopteridae). J Hazard Mater 423:127245

Rosende-Pereiro A, Flores-Ortega JR, González-Sansón G, Corgos A (2020) Stomach content and stable isotopes reveal an ontogenetic dietary shift of young-of-the-year scalloped hammerhead sharks (*Sphyrna lewini*) inhabiting coastal nursery areas. Environ Biol Fishes 103:49–65

Ruppert JLW, Fortin MJ, Meekan MG (2016) The ecological role of sharks on coral reefs: response to Roff et al. Trends Ecol Evol 31:586–587

Sánchez-Hernández J, Nunn AD, Adams CE, Amundsen PA (2019) Causes and consequences of ontogenetic dietary shifts: a global synthesis using fish models. Biol Rev Camb Philos Soc 94:539–554

Shiffman DS, Gallagher AJ, Boyle MD, Hammerschlag-Peyer CM, Hammerschlag N (2012) Stable isotope analysis as a tool for elasmobranch conservation research: a primer for non-specialists. Mar Freshw Res 63:635–643

Shipley ON, Howey LA, Tolentino ER, Jordan LKB, Ruppert JLW, Brooks EJ (2017) Horizontal and vertical movements of Caribbean reef sharks (*Carcharhinus perezi*): conservation implications of limited migration in a marine sanctuary. R Soc Open Sci 4:160611

Skinner C, Mill AC, Newman SP, Newton J, Cobain MRD, Polunin NVC (2019) Novel tri-isotope ellipsoid approach reveals dietary variation in sympatric predators. Ecol Evol 9:13267–13277

Sogawa S, Sugisaki H, Tadokoro K, Ono T, Sato E, Shimode S, Kikuchi T (2017) Feeding habits of six species of euphausiids (Decapoda: Euphausiacea) in the northwestern Pacific Ocean determined by carbon and nitrogen stable isotope ratios. J Crustac Biol 37:29–36

Stehmann MFW (2002) Proposal of a maturity stages scale for oviparous and viviparous cartilaginous fishes (Pisces, Chondrichthyes). Arch Fish Mar Res 50:23–48

Sun M, Li Y, Chen Y (2023) Unveiling unselective fishing in China: a nationwide meta-analysis of multispecies fisheries. Fish Fish 24:142–158

Swanson HK, Lysy M, Power M, Stasko AD, Johnson JD, Reist JD (2015) A new probabilistic method for quantifying n-dimensional ecological niches and niche overlap. Ecology 96:318–324

Teh LSL, Cashion T, Alava Saltos JJ, Cheung WWL, Sumaila UR (2019) Status, trends, and the future of fisheries in the East and South China Seas. Fish Cent Res Rep 27. Institute for the Oceans and Fisheries, The University of British Columbia, Vancouver

Valls M, Rueda L, Quetglas A (2017) Feeding strategies and resource partitioning among elasmobranchs and cephalopods in Mediterranean deep-sea ecosystems. Deep Sea Res I 128:28–41

Vander Zanden MJ, Rasmussen JB (2001) Variation in $\delta^{15}N$ and $\delta^{13}C$ trophic fractionation: implications for aquatic food web studies. Limnol Oceanogr 8:2061–2066

Vaudo JJ, Heithaus MR (2011) Dietary niche overlap in a nearshore elasmobranch mesopredator community. Mar Ecol Prog Ser 425:247–260

Wang Z, Tang H, Xu L, Zhang J (2022) A review on fishing gear in China: selectivity and application. Aquacult Fish 7:345–358

Wetherbee BM, Cortés E (2004) Food consumption and feeding habits. In: Carrier JC, Musick JA, Heithaus MR (eds) Biology of sharks and their relatives. CRC Press, Boca Raton, FL, p 225–246

Xavier JC, Vieira C, Assis C, Cherel Y and others (2012) Ecología alimentaria del tiburón tollo lucero liso *Etmopterus pusillus* (Elasmobranchii: Etmopteridae) en el atlántico nordeste. Sci Mar 76:301–310

Xu Y, Dai X, Huang Z, Sun M, Chen Z, Zhang K (2022) Stock assessment of four dominant shark bycatch species in bottom trawl fisheries in the northern South China Sea. Sustainability 14:3722

Yano T, Ohshimo S, Sakai T, Yoda M (2020) Filling gaps in the biology and habitat use of two spurdog sharks (*Squalus japonicus* and *Squalus brevirostris*) in the East China Sea. Mar Freshw Res 71:1719–1731

Zhang B, Pethybridge H, Sutton C, Virtue P, Li Y (2024) Total mercury concentrations in Tasman Sea mesopelagic fish: exploring biotic and abiotic drivers. Mar Pollut Bull 206: 116676

Zhang S, Jin S, Zhang H, Fan W, Tang F, Yang S (2016) Distribution of bottom trawling effort in the Yellow Sea and East China Sea. PLOS ONE 11:e0166640

Zhang Y, Soerensen AL, Schartup AT, Sunderland EM (2020) A global model for methylmercury formation and uptake at the base of marine food webs. Global Biogeochem Cycles 34:e2019GB006348

Zhang Z (2005) The fishery resources status of sharks in Eastern China Sea. J Fujian Fish 3:10–14

Zheng N, Wang S, Dong W, Hua X and others (2019) The toxicological effects of mercury exposure in marine fish. Bull Environ Contam Toxicol 102:714–720

Zhou F, Hirai J, Hamasaki K, Horii S, Tsuda A (2021) Feeding ecology of three euphausiid species in the North Pacific Ocean inferred from 18S V9 metabarcoding and stable isotope analysis. Front Mar Sci 8:756067

Zou C, Yin D, Wang R (2022) Mercury and selenium bioaccumulation in wild commercial fish in the coastal East China Sea: Selenium benefits versus mercury risks. Mar Pollut Bull 180:113754

Editorial responsibility: Stephen Wing, Dunedin, New Zealand
Reviewed by: A. Rosende-Pereiro, G. Capillo and 2 anonymous referees

Submitted: January 7, 2025
Accepted: July 16, 2025
Proofs received from author(s): October 12, 2025